Applied Physics Letters

Scaling magnetic tunnel junction down to single-digit nanometers—Challenges and prospects

Cite as: Appl. Phys. Lett. **116**, 160501 (2020); https://doi.org/10.1063/5.0004434
Submitted: 12 February 2020 . Accepted: 23 March 2020 . Published Online: 20 April 2020

Butsurin Jinnai, Kyota Watanabe, Shunsuke Fukami, and Hideo Ohno

COLLECTIONS

This paper was selected as Featured

ARTICLES YOU MAY BE INTERESTED IN

Spintronics with compensated ferrimagnets
Applied Physics Letters **116**, 110501 (2020); https://doi.org/10.1063/1.5144076

All-electrical manipulation of magnetization in magnetic tunnel junction via spin-orbit torque
Applied Physics Letters **116**, 162401 (2020); https://doi.org/10.1063/5.0001758

Developing silicon carbide for quantum spintronics
Applied Physics Letters **116**, 190501 (2020); https://doi.org/10.1063/5.0004454

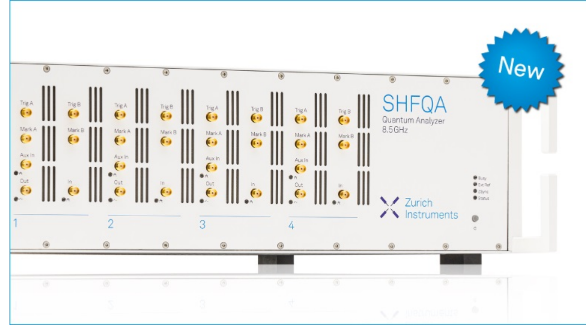

Your Qubits. Measured.
Meet the next generation of quantum analyzers
- Readout for up to 64 qubits
- Operation at up to 8.5 GHz, mixer-calibration-free
- Signal optimization with minimal latency

Find out more

© 2020 Author(s).

Applied Physics Letters PERSPECTIVE scitation.org/journal/apl

Scaling magnetic tunnel junction down to single-digit nanometers—Challenges and prospects

Cite as: Appl. Phys. Lett. **116**, 160501 (2020); doi: 10.1063/5.0004434
Submitted: 12 February 2020 · Accepted: 23 March 2020 ·
Published Online: 20 April 2020

View Online Export Citation CrossMark

Butsurin Jinnai,[1,a)] Kyota Watanabe,[2] Shunsuke Fukami,[1,2,3,4,5] and Hideo Ohno[1,2,3,4,5]

AFFILIATIONS

[1]WPI Advanced Institute for Materials Research, Tohoku University, Sendai 980-8577, Japan
[2]Laboratory for Nanoelectronics and Spintronics, Research Institute of Electrical Communication, Tohoku University, Sendai 980-8577, Japan
[3]Center for Innovative Integrated Electronic Systems, Tohoku University, Sendai 980-0845, Japan
[4]Center for Spintronics Research Network, Tohoku University, Sendai 980-8577, Japan
[5]Center for Science and Innovation in Spintronics, Tohoku University, Sendai 980-8577, Japan

[a)]Author to whom correspondence should be addressed: butsurin@tohoku.ac.jp

ABSTRACT

Magnetic tunnel junction (MTJ), a spintronics device, has been intensively developed in the past couple of decades because of its high potential in terms of non-volatility, fast operation, virtually infinite endurance, scalability, and compatibility with complementary metal-oxide-semiconductor (CMOS) integrated circuits as well as their process and circuits. Today, high-volume manufacturing of spin-transfer torque magnetoresistive random access memory based on MTJ has been initiated for embedded memory applications in CMOS logic. Whether MTJ is scalable along with the advancement of CMOS technology is critical for the technology's future. Here, we review the scaling of MTJ technology, from in-plane anisotropy MTJs to perpendicular interfacial- or shape-anisotropy MTJs. We also discuss challenges and prospects in the future 1X- and X-nm era.

Published under license by AIP Publishing. https://doi.org/10.1063/5.0004434

Spintronics devices hold promise to reduce power consumption and enhance performance in complementary metal-oxide-semiconductor (CMOS) integrated circuits because of their features: non-volatility, fast operation, and high endurance.[1] In the CMOS logic technology, scaling down the feature size to increase the number of devices per unit area, the so-called Moore's law,[2] has been the driving force in the past five decades for technological advancement and exponential economic growth associated with it. While the end of Moore's law may be approaching, the scaling of devices is still the first priority and any device technology that works with the CMOS technology has to prove its scaling capability; spintronics devices are no exception. Indeed, scaling has been one of the main challenges in the development of magnetic tunnel junction (MTJ), a spintronic device, to realize low-power, high-performance, and nonvolatile spin-transfer torque magnetoresistive random access memory (STT-MRAM)[3–5] toward a wide variety of applications such as IoT,[6] automobile,[7] and cryogenic applications,[8] as well as demonstrating its application to CMOS logic.[9,10] As a result of a worldwide effort, we have witnessed significant progress in the MTJ technology.[11–16] The key technology that made today's MTJ is the perpendicular MTJ (p-MTJ) using interfacial anisotropy at a CoFeB/MgO interface,[17] followed by p-MTJs with double-CoFeB/MgO interfaces.[18] Today, high-volume manufacturing of STT-MRAM using the CoFeB/MgO-based interfacial p-MTJs with tens of nanometers has been initiated.[4–7,19–21] Efforts continue to further scale p-MTJ.[22,23] Here, we first review the requirements that the MTJ technology needs to satisfy for nonvolatile memory applications, followed by the recent advancements in the MTJ scaling, and then discuss challenges and prospects that await the technology in the future.

An MTJ is a thin film stack structure that has two ferromagnetic layers (free and reference layers) separated by an insulating tunnel barrier (Fig. 1).[24] In the MTJ, information is stored as the relative alignment of the magnetization orientations of the two layers, which is read via the tunnel magnetoresistance (TMR).[25,26] To write information, the magnetization orientation of the free layer is switched by spin-transfer torque (STT);[27,28] there is an intrinsic critical current I_{C0}

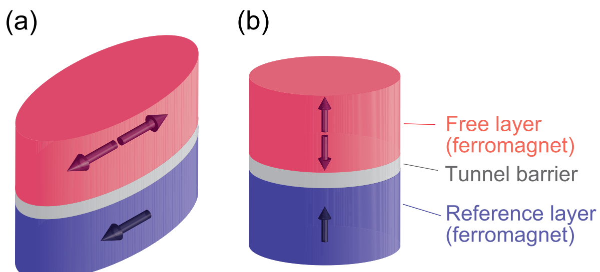

FIG. 1. MTJ structure consists of two ferromagnetic layers (free and reference layers) separated by a tunnel barrier insulator. (a) In-plane configuration with an elliptical shape and (b) perpendicular configuration with a circular shape. Whereas the magnetization orientation in the reference layer is fixed, that in the free layer can be switched by spin-transfer torques (STTs).

above which the free layer changes its magnetization direction according to the polarity of the current. Device performance of an MTJ is first characterized by the TMR ratio, I_{C0}, and the thermal stability factor Δ ($=E/k_BT$, where E is the energy barrier between the two magnetization configurations, k_B is the Boltzmann constant, and T is an absolute temperature); they determine the read, write, and retention performance, respectively. The TMR ratio is defined as $(R_{AP} - R_P)/R_P$, where $R_{AP(P)}$ is the resistance with the antiparallel (parallel) magnetization alignment. The requirement of TMR ratio is determined by the read margin [=TMR ratio/$\sigma(R_P)$, where $\sigma(R_P)$ is the R_P distribution of device arrays], which is typically required to be 20 or higher for reliable and fast read operation.[6] For example, if $\sigma(R_P)$ is 5%, TMR ratio needs to be higher than 100%. The I_{C0} is directly linked to the write power consumption, given as $I_{C0} = (2\alpha\gamma e/\mu_B g_{STT})E$, where α is the damping constant, γ is the gyromagnetic ratio, e is the elementary charge, μ_B is the Bohr magneton, and g_{STT} is the STT efficiency.[27,28] Low I_{C0} is also desirable to achieve a small footprint of the required cell transistor, which is crucial for high-density STT-MRAM because the transistor size is also a limiting factor to scaling its bit density.[11] For high-speed switching at sub-10 ns, the switching current increases beyond I_{C0}, entering the precessional magnetization switching regime.[29,30] I_{C0} is translated into critical switching voltage V_{C0} ($=J_{C0}RA$), where J_{C0} is the intrinsic critical current density and RA is the resistance (R)-area (A) product that exponentially increases with the thickness of the insulating tunnel barrier. V_{C0} needs to be well below the supply voltage in the CMOS circuit, typically 1 V, because the supply voltage is divided by an MTJ and a cell transistor. For high-density standalone memory applications capable of 10-year retention, Δ of 80 or higher at room temperature is required,[31] although the Δ requirement varies with the distribution of device characteristics and the operation range of temperature. It is important to accurately determine Δ for nonvolatile application.[32–34] The values of Δ, or E, of an MTJ experimentally obtained depend on the models describing dominant magnetization reversal mode, which shows a transition from domain-wall propagation to single-domain reversal with the decrease in the MTJ size.[35,36] The critical size of the transition is determined by magnetic parameters such as the exchange stiffness constant and the effective anisotropy energy density K_{eff} of the device, and thus understanding of such parameters[37–40] is important to determine E. For MTJs described by the single-domain reversal model, E is written as $E = K_{eff}tA$, where t is the free-layer thickness. This leads to the necessity to increase $K_{eff}t$ against the area reduction in order to ensure sufficient Δ as the MTJ size shrinks. It should also be noted that keeping or reducing the J_{C0} proportional to $K_{eff}t$ while meeting the Δ requirement is one of the key challenges in the MTJ scaling. For applications that require preprogramming data, data need to be retained during the reflow-soldering process that reaches up to 260 °C,[41] which can be translated into 10-year retention at 225 °C or higher.[42] In addition, MTJs for embedded applications have to be compatible with the CMOS back-end-of-line (BEOL) processes, i.e., robust against the thermal budget, typically 400 °C or higher. Meeting all the above-mentioned requirements concurrently is crucial for MTJ applications in embedded and stand-alone STT-MRAM and other applications.

The first observation of STT-induced magnetization switching in MTJ[43] was with in-plane magnetization [Fig. 1(a)]; the magnetization easy axis is in the film plane by making the shape of the magnet elliptical using the shape anisotropy. Switching efficiency, given by Δ/I_{C0}, is low because the energy E involved in I_{C0} in in-plane configuration is determined by the demagnetizing energy orders of magnitude higher than the in-plane anisotropy energy that determines Δ.[44] To overcome this, perpendicular-magnetization configuration was investigated [Fig. 1(b)],[45] where both Δ and I_{C0} are governed by the same perpendicular anisotropy, providing a route to high Δ/I_{C0} with high Δ and low I_{C0}. In this case, the shape of the magnet can be made circular because the p-MTJs no longer rely on the shape for anisotropy.

While there were early reports on STT switching in p-MTJs,[46–48] the search of a perpendicular material system suitable for high-performance MTJ was regarded as challenges[49] until the report on CoFeB/MgO p-MTJs with reduced CoFeB thickness [Fig. 2(a)].[17] The CoFeB/MgO material system had been a standard material system for *in-plane* MTJs with high TMR ratio,[50–52] which originates from tunneling characteristics involved in crystalline (001) CoFe with (001) MgO.[53,54] The crystalline structure is obtained by annealing of initially amorphous CoFeB and highly (001) oriented MgO, a solid-phase epitaxy of CoFeB with the adjacent highly (001) oriented MgO layer as a template.[50,51] Boron absorption at the side opposite to the CoFeB/MgO interface was found critical.[55,56] While many searched material

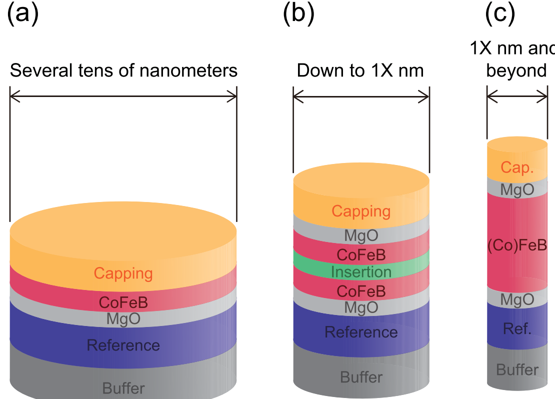

FIG. 2. Evolution of the perpendicular MTJ (p-MTJ) material stack for the MTJ scaling. (a) Interfacial p-MTJ with a single CoFeB/MgO interface. (b) Interfacial p-MTJ with double CoFeB/MgO interfaces and an insertion layer. (c) Shape-anisotropy p-MTJ. Reference layers use synthetic ferrimagnetic layers to compensate for a shift field.

Published under license by AIP Publishing

systems result in perpendicular anisotropy for p-MTJ, it was discovered that CoFeB/MgO itself can produce perpendicular easy-axis if one makes the CoFeB free layer thin enough; the interfacial perpendicular anisotropy at the CoFeB/MgO interface overcomes the in-plane shape anisotropy, leading to perpendicular easy axis.[57] The initial p-MTJ using the CoFeB/MgO material system showed that it satisfies the requirements to a level that had not been possible in earlier attempts: TMR ratio of 120%, Δ of 43, and I_{C0} of 49 μA at 40 nm in diameter.[17] Fast switching speed down to 1 ns[58] and low write error rate below 10^{-11}[59] were also demonstrated. These results clearly showed the potential of the material system and the route toward MTJ scaling.[60–62] The use of the well-studied CoFeB/MgO system helped to accelerate the development of the p-MTJ technology.

The Δ realized in these early p-MTJs was not high enough. In order to increase Δ while continuing the scaling, one needs to enhance $K_{eff}t$. Δ is linearly proportional to t when the MTJs are assumed to follow the nucleation model.[63] However, increasing t makes the in-plane shape anisotropy larger and thus the perpendicular easy axis is compromised. To maintain the perpendicular easy axis while increasing t, double CoFeB/MgO interface structure was employed. To enhance the interfacial anisotropy, a thin insertion layer of heavy metals, such as Ta,[18] Mo,[64] or W,[65] thin enough to exchange couple the separated free layers, was inserted in the CoFeB free layer [Fig. 2(b)]to extract boron from the CoFeB/MgO interfaces during annealing, resulting in high interfacial anisotropy. The double-MgO structure having the insertion layer doubles Δ without increasing I_{C0} compared with the single-MgO structure, an improvement in Δ/I_{C0} by a factor of two.[18,66] This improvement was attributed to the reduction in α[67] through the suppression of spin pumping by the MgO layers.[68,69] Double-MgO structure allowed the scaling down to and beyond 20 nm in diameter with good performance.[66,70–73] Along with the advancements in the free layer, a reference layer with synthetic ferrimagnetic layers based on Co/Pt multilayers was developed to compensate for a dipolar field to the free layer.[74,75] Given the advantages in the p-MTJs with the double-MgO structure having the boron-absorbing insertion layer, it has become a *de facto* standard structure for today's STT-MRAM in high-volume manufacturing.[4–7,19–21]

As an extension of the p-MTJs with the double-MgO structure, p-MTJs having three MgO layers, or quad interfaces, was recently demonstrated; Δ in the quad-interface structure was 1.5–2 times higher than that with the double-MgO structure without an increase in I_{C0}.[23,76]

The interfacial-anisotropy p-MTJs have paved the way beyond 20 nm. Further scaling capability of MTJs beyond 1X nm was demonstrated recently. In the interfacial-anisotropy p-MTJs Δ is, for the first approximation, proportional to the area of the CoFeB/MgO interface, and as such becomes insufficient when the area is reduced.[77,78] The shape-anisotropy p-MTJs have been shown to overcome this shortcoming.[22] $K_{eff}t$ is expressed as $K_{eff}t = K_b t + K_i - \delta N M_S^2 t/2\mu_0$, where K_b is the bulk anisotropy density, K_i is the interfacial anisotropy density, M_S is the spontaneous magnetization, μ_0 is the permeability in free space, and δN is the difference in dimensionless demagnetization coefficient, or the shape anisotropy coefficient, between the perpendicular and in-plane orientations. Figure 3(a) shows the δN with respect to the cross-sectional aspect ratio t/D of the magnet in the free layer. The shape anisotropy $-\delta N M_S^2 t/2\mu_0$ with a disk-shaped free layer ($t/D < 1$ and $\delta N > 0$) favors an in-plane easy axis, but that with a bar-shaped free layer ($t/D > 1$ and $\delta N < 0$) enhances the perpendicular anisotropy (a bar magnet!). Figure 3(b) shows the design window for the magnet shape in the free layer regarding Δ and V_{C0}, assuming that $RA = 1\,\Omega\,\mu m^2$.[22] The red- and blue-hatched regions indicate $\Delta \geq 80$ and $V_{C0} \leq 0.5$ V, respectively. The overlapped regions indicate a favorable design window of the shape of the free-layer magnet to achieve highly reliable and low-power STT-MRAM. The overlapped regions below $t = 3$ nm and above $t = 14$ nm correspond to the p-MTJs based

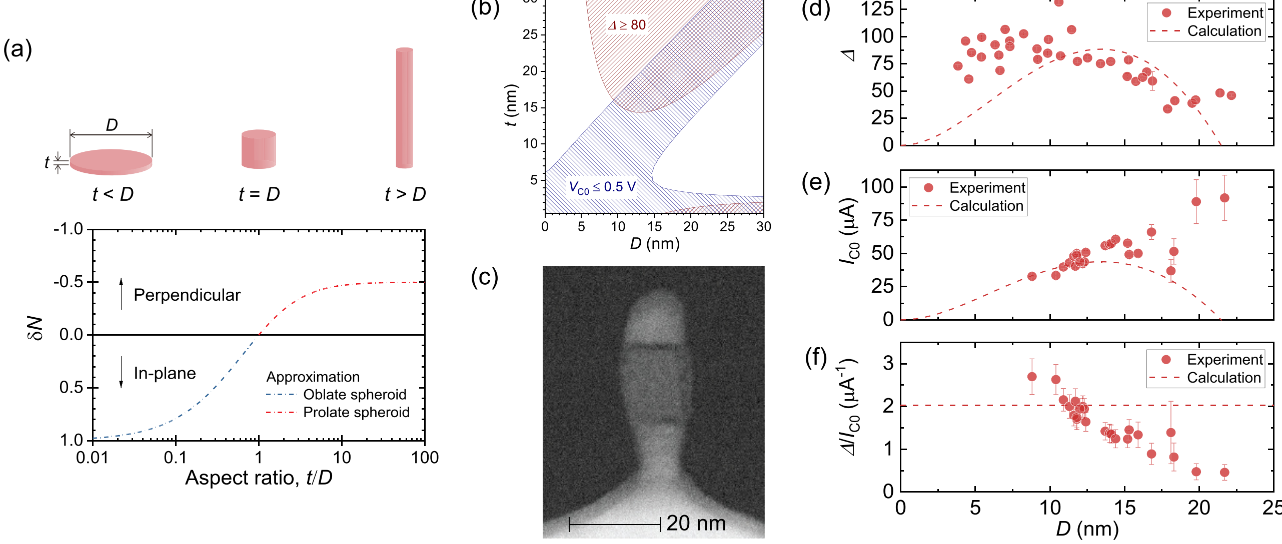

FIG. 3. (a) Aspect ratio t/D dependence of the difference in dimensionless demagnetization coefficient δN. (b) Design window for the magnet shape in the free layer (t and D). (c) Cross-sectional high-angle annular dark-field scanning transmission electron microscopy for the patterned MTJ with a thick FeB layer sandwiched by MgO layers. (d)–(f) Properties of the shape-anisotropy p-MTJs: the D dependences of (d) Δ, (e) I_{C0}, and (f) Δ/I_{C0}. (a)–(c) are reprinted from Watanabe *et al.*, Nat. Commun. **9**, 663 (2018).[22] Copyright 2018 Author(s), licensed under a Creative Commons Attribution (CC BY) license.

on the interfacial anisotropy and the shape anisotropy, respectively. One can see that the interfacial-anisotropy p-MTJs limit the scaling down to around 15 nm, whereas the shape-anisotropy p-MTJs can continue below 10 nm.

The first demonstration of this concept involved a stack similar to the interfacial-anisotropy p-MTJs with the double-MgO structure except for the thickness of the FeB ferromagnet in the free layer [Fig. 2(c)] and showed that indeed it is possible to have good performance at device size of single-digit nanometers.[22] Figure 3(c) shows a thick FeB free layer sandwiched by MgO layers with $D \sim 10$ nm and $t \sim 15$ nm observed using cross-sectional high-angle annular dark-field scanning transmission electron microscopy for a patterned MTJ.[22] Figures 3(d) and 3(e) are the measured Δ and I_{C0}, and Fig. 3(f) is the corresponding switching efficiency Δ/I_{C0}. Broken lines represent calculation based on an analytical model of the shape-anisotropy p-MTJ.[22] Δ increases as D shrinks because $-\delta N$ increases. Further reduction of D results in lowering Δ because of the volume reduction. Yet, the shape-anisotropy p-MTJs with $RA = 4.5\,\Omega\,\mu m^2$ exhibit high Δ below 10 nm; $\Delta = 73$ at the smallest studied diameter $D = 3.8$ nm. Current-induced magnetization switching was observed down to $D = 8.8$ nm. While higher Δ was obtained with the shape-anisotropy p-MTJs, the obtained Δ/I_{C0} was comparable with the interfacial-anisotropy p-MTJs with the double-MgO structure having diameters of 1X nm.[70] The difference between experiment and calculation in I_{C0} may be related to the device edge affected by fabrication processes.[40,79]

Figure 4 is the summary of the experimentally measured representative Δ at room temperature of p-MTJs reported to date: the interfacial-anisotropy p-MTJs with the single-[17,58,60–62] and double-MgO structures,[18,70,80–82] and the shape-anisotropy p-MTJs[22,83] are all included. Note that the methods of Δ measurement in Fig. 4 differ by the reports; Δ values for large MTJs, where the single-domain reversal model is no longer effective, may vary depending on the assumption of magnetization-reversal models, such as nucleation[60] and domain-propagation models.[35,36] The interfacial-anisotropy p-MTJs with the double-MgO structure achieve high Δ down to 20 nm but so far not beyond. The shape-anisotropy p-MTJs show scaling down to single-digit nanometers, or X nm, while maintaining high enough thermal stability. Along with the scalability, the shape-anisotropy p-MTJs also allows one to explore free-layer material because the free layer is thick; one can adopt materials possessing high M_S, not limited to (Co)FeB-based materials; the shape-anisotropy p-MTJs using the different material systems, such as NiFe and Co, were successfully fabricated.[83]

Next, we discuss issues and challenges that need to be addressed for further development of the MTJ technology; here, we focus on the shape-anisotropy p-MTJ.

In a nanoscale bar-shaped ferromagnet, an upper limit of thickness t, and hence Δ,[83] is related to domain wall width δ_{DW} to realize coherent reversal. While it is preferable to maintain $t < \delta_{DW}$, multilayer structures might offer a design window in which an increase in Δ is realized without triggering incoherent reversal.

For application, reduction of V_{C0}, which is now > 0.5 V, needs to be explored. Reduction of I_{C0} may be possible by employing a material with low α while maintaining Δ with high M_S and perhaps simultaneously utilizing bulk anisotropy. Achieving low RA also reduces V_{C0}. This requires reduction of MgO thickness while avoiding MgO break down and maintaining a high TMR ratio. The lower bound of the MgO thickness was reported to be three monolayers.[84] Physics involved in this minimum thickness need to be investigated to further reduce the thickness.

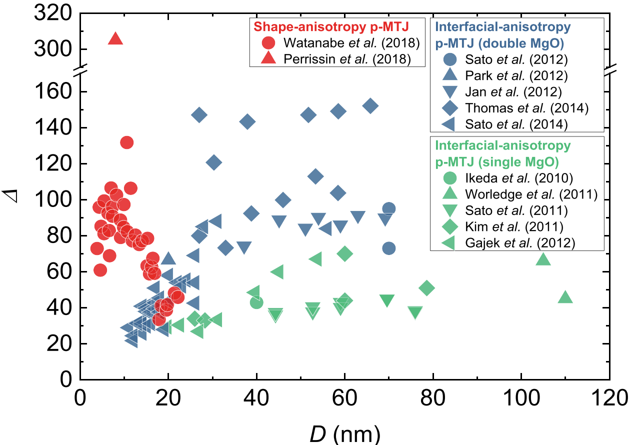

FIG. 4. Δ at room temperature plotted with respect to D for the various p-MTJs. Data for the interfacial-anisotropy p-MTJs with the single-MgO structure are taken from Ikeda *et al.*, Nat. Mater. **9**, 721 (2010) (Ref. 17); Worledge *et al.*, Appl. Phys. Lett. **98**, 022501 (2011) (Ref. 58); Sato *et al.*, Appl. Phys. Lett. **99**, 042501 (2011) (Ref. 60); Kim *et al.*, IEEE IEDM **2011**, 24.1.1 (Ref. 61); and Gajek *et al.*, Appl. Phys. Lett. **100**, 132408 (2012) (Ref. 62). Data for the interfacial-anisotropy p-MTJs with the double-MgO structure are taken from Sato *et al.*, Appl. Phys. Lett. **101**, 022414 (2012) (Ref. 18); Park *et al.*, VLSI Symposium (2012), p. 57 (Ref. 80); Jan *et al.*, Appl. Phys. Express **5**, 093008 (2012) (Ref. 81); Thomas *et al.*, J. Appl. Phys. **115**, 172615 (2014) (Ref. 82); and Sato *et al.*, Appl. Phys. Lett. **105**, 062403 (2014) (Ref. 70). Data for the shape-anisotropy p-MTJs are taken from Watanabe *et al.*, Nat. Commun. **9**, 663 (2018) (Ref. 22) and Perrissin *et al.*, Nanoscale **10**, 12187 (2018) (Ref. 83). Data are reproduced with permission from Sato *et al.*, Appl. Phys. Lett. **99**, 042501 (2011). Copyright 2011 AIP Publishing LLC; Kim *et al.*, IEEE IEDM **2011**, 24.1.1. Copyright 2011 IEEE; Gajek *et al.*, Appl. Phys. Lett. **100**, 132408 (2012). Copyright 2012 AIP Publishing LLC; Park *et al.*, VLSI Symposium (2012), p. 57. Copyright 2012 IEEE; Thomas *et al.*, J. Appl. Phys. **115**, 172615 (2014) and Sato *et al.*, Appl. Phys. Lett. **105**, 062403 (2014). Copyright 2014 AIP Publishing LLC; and Watanabe *et al.*, Nat. Commun. **9**, 663 (2018). Copyright 2018 Author(s), licensed under a CC BY license.

One needs to come up with a scheme to reduce interference among densely packed MTJs. This is particularly true for shape-anisotropy p-MTJs, as the shape anisotropy contribution to Δ is proportional to M_S of the employed material, which generates dipolar fields. For example, based on the demonstrated shape-anisotropy p-MTJs with 3.8-nm diameter,[22] dipolar fields decay to less than 10% of the coercive field of 110 mT at the distance of 8 nm from the dot edge. This means that the effect on data retention may become an issue when the pitch of device array becomes two times device diameter. The effect on the magnetization dynamics for ultrafast switching[85] should also be investigated.

Finally, developing means for MTJ patterning, particularly high-density array patterning, is of paramount importance for applications. Unlike silicon patterning that uses reactive ion etching (RIE), ion beam etching (IBE) is often used for MTJ patterning because of low volatility of etching byproducts and vulnerability of magnetic materials to chemical reaction with etching gases. For the fabrication of the shape-anisotropy p-MTJs, multi-step IBE with various incident angles was used.[22,83] This process is only possible for an isolated MTJ in open space but not applicable to dense pattern with narrow pitch. Also,

edge degradation during integration processes needs to be understood and minimized. High-energy ion beam during IBE affects the magnetic stack integrity, and chemical species exposed during the following passivation deposition, such as hydrogen, nitrogen, and oxygen, are prone to react with the surface of magnetic materials.[3] The device performance degradation in Fig. 3(e) and the difference between physically measured and electrically determined diameters[22,62] may be a result of the fabrication process. As the MTJ size shrinks, the understanding of the properties of the affected parts and their role on device performance becomes increasingly important.[40,79,86,87] Size variation and/or edge roughness induced by the patterning processes is another general but critical issue in single-digit nanometer MTJs to ensure a required operation margin. For example, if one has 4-nm MTJs with the size variation of ± 0.4 nm ($\pm 10\%$), the TMR ratio of 400% or higher is necessary for the read margin of 20. Given the challenges, fine-control and low-damage fabrication process is indispensable and the development of such manufacturing technology will play a more important role than ever for the MTJ technology.

We have reviewed the MTJ technology focusing on its scaling. Since the first demonstration of the p-MTJs using the CoFeB/MgO interfacial anisotropy with 40 nm in diameter,[17] scaling has been the central issue for technology. Today, the p-MTJs with the double CoFeB/MgO interfaces and the insertion layer[18] provide high-performance MTJ.[3–7,19–21,88–91] As an extension, the p-MTJs with quad interfaces revealed to have high enough performance for scaling down to 1X nm.[23] The shape-anisotropy p-MTJs achieved scaling to single-digit nanometers.[22,83] In the MTJ scaling technology, challenges remain particularly in the fabrication front, i.e., integration processes. It is important to note that, for high-speed switching below a few nanoseconds, spin–orbit torque (SOT)[92–94] switching offers another promising route with reasonably small I_{C0},[95] although it is larger than that of STT switching at a timescale longer than a few tens of nanoseconds. For the SOT switching of a perpendicular or an in-plane-collinear magnetization,[94] I_{C0} is independent of α,[96,97] allowing further material flexibility. Just like DRAM and SRAM, both STT and SOT devices, once the technology matures, may be used to fulfill different requirements and needs. Offering non-volatility, fast operation, virtually infinite endurance, scalability, and CMOS compatibility at the same time, spintronics devices are on their way to becoming an indispensable ingredient for CMOS technology to make it low-power and high-performance in the century of data.

The authors would like to thank H. Sato, S. Kanai, Y. Takeuchi, J. Igarashi, and T. Funatsu for their fruitful discussion. This work was partly supported by JST-OPERA Grant No. JPMJOP1611, Cooperative Research Projects of RIEC, and JSPS KAKENHI Grant No. JP19K04486.

The data that support the findings of this study are available from the corresponding author upon reasonable request.

REFERENCES

[1]H. Ohno, T. Endoh, T. Hanyu, N. Kasai, and S. Ikeda, in IEEE International Electron Devices Meeting (2010), pp. 9.4.1–9.4.4.
[2]G. E. Moore, Electronics **38**, 114 (1965); Proc. IEEE **86**, 82 (1998).
[3]H. Sato, H. Honjo, T. Watanabe, M. Niwa, H. Koike, S. Miura, T. Saito, H. Inoue, T. Nasuno, T. Tanigawa, Y. Noguchi, T. Yoshiduka, M. Yasuhira, S. Ikeda, S.-Y. Kang, T. Kubo, K. Yamashita, Y. Yagi, R. Tamura, and T. Endoh, in IEEE International Electron Devices Meeting (2018), pp. 27.2.1–27.2.4.
[4]S. Aggarwal, H. Almasi, M. DeHerrera, B. Hughes, S. Ikegawa, J. Janesky, H. K. Lee, H. Lu, F. B. Mancoff, K. Nagel, G. Shimon, J. J. Sun, T. Andre, S. M. Alam, B. Y. Seo, S. H. Han, Y. Ji, H. T. Jung, S. O. Park, O. I. Kwon, J. W. Kye, Y. D. Kim, S. W. Pae, Y. J. Song, G. T. Jeong, K. H. Hwang, G. H. Koh, H. K. Kang, and E. S. Jung, in IEEE International Electron Devices Meeting (2019), pp. 2.1.1–2.1.4.
[5]K. Lee, J. H. Bak, Y. J. Kim, C. K. Kim, A. Antonyan, D. H. Chang, S. H. Hwang, G. W. Lee, N. Y. Ji, W. J. Kim, J. H. Lee, B. J. Bae, J. H. Park, I. H. Kim, B. Y. Seo, S. H. Han, Y. J. Ji, H. T. Jung, S. O. Park, O. I. Kwon, J. W. Kye, Y. D. Kim, S. W. Pae, Y. J. Song, G. T. Jeong, K. H. Hwang, G. H. Koh, H. K. Kang, E. S. Jung, S. L. Tan, C. S. Seet, Y. S. You, S. T. Woo, E. Quek, S. Y. Siah, and J. Pellerin, in IEEE International Electron Devices Meeting (2019), pp. 2.2.1–2.2.4.
[6]V. B. Naik, K. Lee, K. Yamane, R. Chao, J. Kwon, N. Thiyagarajah, N. L. Chuang, S. H. Jang, B. Behin-Aein, J. H. Lim, T. Y. Lee, W. P. Neo, H. Dixit, S. K. C. Goh, T. Ling, J. Hwang, D. Zeng, J. W. Ting, E. H. Toh, L. Zhang, R. Low, N. Balasankaran, L. Y. Zhang, K. W. Gan, L. Y. Hau, J. Mueller, B. Pfefferling, O. Kallensee, S. L. Tan, C. S. Seet, Y. S. You, S. T. Woo, E. Quek, S. Y. Siah, and J. Pellerin, in IEEE International Electron Devices Meeting (2019), pp. 2.3.1–2.3.4.
[7]W. J. Gallagher, E. Chien, T.-W. Chiang, J.-C. Huang, M.-C. Shih, C. Y. Wang, C.-H. Weng, S. Chen, C. Bair, G. Lee, Y.-C. Shih, C.-F. Lee, P.-H. Lee, R. Wang, K.-H. Shen, J. J. Wu, W. Wang, and H. Chuang, in IEEE International Electron Devices Meeting (2019), pp. 2.7.1–2.7.4.
[8]L. Rehm, G. Wolf, B. Kardasz, M. Pinarbasi, and A. D. Kent, Appl. Phys. Lett. **115**, 182404 (2019).
[9]S. Matsunaga, J. Hayakawa, S. Ikeda, K. Miura, H. Hasegawa, T. Endoh, H. Ohno, and T. Hanyu, Appl. Phys. Express **1**, 091301 (2008).
[10]T. Hanyu, T. Endoh, D. Suzuki, H. Koike, Y. Ma, N. Onizawa, M. Natsui, S. Ikeda, and H. Ohno, Proc. IEEE **104**, 1844 (2016).
[11]T. Kawahara, K. Ito, R. Takemura, and H. Ohno, Microelectron. Reliab. **52**, 613 (2012).
[12]A. Brataas, A. D. Kent, and H. Ohno, Nat. Mater. **11**, 372 (2012).
[13]A. D. Kent and D. C. Worledge, Nat. Nanotechnol. **10**, 187 (2015).
[14]D. Apalkov, B. Dieny, and J. M. Slaughter, Proc. IEEE **104**, 1796 (2016).
[15]B. Dieny and M. Chshiev, Rev. Mod. Phys. **89**, 025008 (2017).
[16]S. Bhatti, R. Sbiaa, A. Hirohata, H. Ohno, S. Fukami, and S. N. Piramanayagam, Mater. Today **20**, 530 (2017).
[17]S. Ikeda, K. Miura, H. Yamamoto, K. Mizunuma, H. D. Gan, M. Endo, S. Kanai, J. Hayakawa, F. Matsukura, and H. Ohno, Nat. Mater. **9**, 721 (2010).
[18]H. Sato, M. Yamanouchi, S. Ikeda, S. Fukami, F. Matsukura, and H. Ohno, Appl. Phys. Lett. **101**, 022414 (2012).
[19]J. J. Kan, C. Park, C. Ching, J. Ahn, L. Xue, R. Wang, A. Kontos, S. Liang, M. Bangar, H. Chen, S. Hassan, S. Kim, M. Pakala, and S. H. Kang, in IEEE International Electron Devices Meeting (2016), pp. 27.4.1–27.4.4.
[20]L. Xue, C. Ching, A. Kontos, J. Ahn, X. Wang, R. Whig, H. Tseng, J. Howarth, S. Hassan, H. Chen, M. Bangar, S. Liang, R. Wang, and M. Pakala, in IEEE Symposium on VLSI Technology (2018), pp. 117–118.
[21]J. G. Alzate, U. Arslan, P. Bai, J. Brockman, Y. J. Chen, N. Das, K. Fischer, T. Ghani, P. Heil, P. Hentges, R. Jahan, A. Littlejohn, M. Mainuddin, D. Ouellette, J. Pellegren, T. Pramanik, C. Puls, P. Quintero, T. Rahman, M. Sekhar, B. Sell, M. Seth, A. J. Smith, A. K. Smith, L. Wei, C. Wiegand, O. Golonzka, and F. Hamzaoglu, in IEEE International Electron Devices Meeting (2019), pp. 2.4.1–2.4.4.
[22]K. Watanabe, B. Jinnai, S. Fukami, H. Sato, and H. Ohno, Nat. Commun. **9**, 663 (2018).
[23]K. Nishioka, H. Honjo, S. Ikeda, T. Watanabe, S. Miura, H. Inoue, T. Tanigawa, Y. Noguchi, M. Yasuhira, H. Sato, and T. Endoh, in IEEE Symposium on VLSI Technology (2019), pp. T120–T121.
[24]M. Julliere, Phys. Lett. A **54**, 225 (1975).
[25]T. Miyazaki and N. Tezuka, J. Magn. Magn. Mater. **139**, L231 (1995).
[26]J. S. Moodera, L. R. Kinder, T. M. Wong, and R. Meservey, Phys. Rev. Lett. **74**, 3273 (1995).
[27]J. C. Slonczewski, J. Magn. Magn. Mater. **159**, L1 (1996).
[28]L. Berger, Phys. Rev. B **54**, 9353 (1996).
[29]M. Hosomi, H. Yamagishi, T. Yamamoto, K. Bessho, Y. Higo, K. Yamane, H. Yamada, M. Shoji, H. Hachino, C. Fukumoto, H. Nagao, and H. Kano, in IEEE International Electron Devices Meeting (2005), pp. 459–462.

Published under license by AIP Publishing

[30]Z. Diao, Z. Li, S. Wang, Y. Ding, A. Panchula, E. Chen, L.-C. Wang, and Y. Huai, J. Phys. Condens. Matter 19, 165209 (2007).
[31]R. Takemura, T. Kawahara, K. Miura, H. Yamamoto, J. Hayakawa, N. Matsuzaki, K. Ono, M. Yamanouchi, K. Ito, H. Takahashi, S. Ikeda, H. Hasegawa, H. Matsuoka, and H. Ohno, IEEE J. Solid-State Circuits 45, 869 (2010).
[32]W. Rippard, R. Heindl, M. Pufall, S. Russek, and A. Kos, Phys. Rev. B 84, 064439 (2011).
[33]M. Bersweiler, H. Sato, and H. Ohno, IEEE Magn. Lett. 8, 3109003 (2017).
[34]E. C. I. Enobio, M. Bersweiler, H. Sato, S. Fukami, and H. Ohno, Jpn. J. Appl. Phys., Part 1 57, 04FN08 (2018).
[35]G. D. Chaves-O'Flynn, G. Wolf, J. Z. Sun, and A. D. Kent, Phys. Rev. Appl. 4, 024010 (2015).
[36]L. Thomas, G. Jan, S. Le, Y. J. Lee, H. Liu, J. Zhu, S. Serrano-Guisan, R. Y. Tong, K. Pi, D. Shen, R. He, J. Haq, Z. Teng, R. Annapragada, V. Lam, Y. J. Wang, T. Zhong, T. Torng, and P. K. Wang, in IEEE International Electron Devices Meeting (2015), pp. 26.4.1–26.4.4.
[37]N. Ichikawa, T. Dohi, A. Okada, H. Sato, S. Fukami, and H. Ohno, Appl. Phys. Lett. 112, 202402 (2018).
[38]J. B. Mohammadi, B. Kardasz, G. Wolf, Y. Chen, M. Pinarbasi, and A. D. Kent, ACS Appl. Electron. Mater. 1, 2025 (2019).
[39]K. Mizunuma, M. Yamanouchi, H. Sato, S. Ikeda, S. Kanai, F. Matsukura, and H. Ohno, Appl. Phys. Express 6, 063002 (2013).
[40]M. Shinozaki, J. Igarashi, H. Sato, and H. Ohno, Appl. Phys. Express 11, 043001 (2018).
[41]See https://www.jedec.org/system/files/docs/J-STD-020E.pdf for JEDEC, J-STD-020E (2014).
[42]W. J. Gallagher, E. Chien, T. Chiang, J. Huang, M. Shih, C. Y. Wang, C. Bair, G. Lee, Y. Shih, C. Lee, R. Wang, K. Shen, J. J. Wu, W. Wang, and H. Chuang, in IEEE Symposium on VLSI Technology (2019), pp. T190–T191.
[43]Y. Huai, F. Albert, P. Nguyen, M. Pakala, and T. Valet, Appl. Phys. Lett. 84, 3118 (2004).
[44]J. Z. Sun, Phys. Rev. B 62, 570 (2000).
[45]S. Mangin, D. Ravelosona, J. A. Katine, M. J. Carey, B. D. Terris, and E. E. Fullerton, Nat. Mater. 5, 210 (2006).
[46]M. Nakayama, T. Kai, N. Shimomura, M. Amano, E. Kitagawa, T. Nagase, M. Yoshikawa, T. Kishi, S. Ikegawa, and H. Yoda, J. Appl. Phys. 103, 07A710 (2008).
[47]T. Kishi, H. Yoda, T. Kai, T. Nagase, E. Kitagawa, M. Yoshikawa, K. Nishiyama, T. Daibou, M. Nagamine, M. Amano, S. Takahashi, M. Nakayama, N. Shimomura, H. Aikawa, S. Ikegawa, S. Yuasa, K. Yakushiji, H. Kubota, A. Fukushima, M. Oogane, T. Miyazaki, and K. Ando, in IEEE International Electron Devices Meeting (2008), pp. 1–4.
[48]H. Yoda, T. Kishi, T. Nagase, M. Yoshikawa, K. Nishiyama, E. Kitagawa, T. Daibou, M. Amano, N. Shimomura, S. Takahashi, T. Kai, M. Nakayama, H. Aikawa, S. Ikegawa, M. Nagamine, J. Ozeki, S. Mizukami, M. Oogane, Y. Ando, S. Yuasa, K. Yakushiji, H. Kubota, Y. Suzuki, Y. Nakatani, T. Miyazaki, and K. Ando, Curr. Appl. Phys. 10, e87 (2010).
[49]S. Ikeda, H. Sato, M. Yamanouchi, H. Gan, K. Miura, K. Mizunuma, S. Kanai, S. Fukami, F. Matsukura, N. Kasai, and H. Ohno, SPIN 02, 1240003 (2012).
[50]D. D. Djayaprawira, K. Tsunekawa, M. Nagai, H. Maehara, S. Yamagata, N. Watanabe, S. Yuasa, Y. Suzuki, and K. Ando, Appl. Phys. Lett. 86, 092502 (2005).
[51]J. Hayakawa, S. Ikeda, F. Matsukura, H. Takahashi, and H. Ohno, Jpn. J. Appl. Phys., Part 2 44, L587 (2005).
[52]S. Ikeda, J. Hayakawa, Y. Ashizawa, Y. M. Lee, K. Miura, H. Hasegawa, M. Tsunoda, F. Matsukura, and H. Ohno, Appl. Phys. Lett. 93, 082508 (2008).
[53]W. H. Butler, X.-G. Zhang, T. C. Schulthess, and J. M. MacLaren, Phys. Rev. B 63, 054416 (2001).
[54]J. Mathon and A. Umerski, Phys. Rev. B 63, 220403 (2001).
[55]S. V. Karthik, Y. K. Takahashi, T. Ohkubo, K. Hono, S. Ikeda, and H. Ohno, J. Appl. Phys. 106, 023920 (2009).
[56]Z. Wang, M. Saito, K. P. McKenna, S. Fukami, H. Sato, S. Ikeda, H. Ohno, and Y. Ikuhara, Nano Lett. 16, 1530 (2016).
[57]M. Endo, S. Kanai, S. Ikeda, F. Matsukura, and H. Ohno, Appl. Phys. Lett. 96, 212503 (2010).
[58]D. C. Worledge, G. Hu, D. W. Abraham, J. Z. Sun, P. L. Trouilloud, J. Nowak, S. Brown, M. C. Gaidis, E. J. O'Sullivan, and R. P. Robertazzi, Appl. Phys. Lett. 98, 022501 (2011).
[59]J. J. Nowak, R. P. Robertazzi, J. Z. Sun, G. Hu, D. W. Abraham, P. L. Trouilloud, S. Brown, M. C. Gaidis, E. J. O'Sullivan, W. J. Gallagher, and D. C. Worledge, IEEE Magn. Lett. 2, 3000204 (2011).
[60]H. Sato, M. Yamanouchi, K. Miura, S. Ikeda, H. D. Gan, K. Mizunuma, R. Koizumi, F. Matsukura, and H. Ohno, Appl. Phys. Lett. 99, 042501 (2011).
[61]W. Kim, J. H. Jeong, Y. Kim, W. C. Lim, J. H. Kim, J. H. Park, H. J. Shin, Y. S. Park, K. S. Kim, S. H. Park, Y. J. Lee, K. W. Kim, H. J. Kwon, H. L. Park, H. S. Ahn, S. C. Oh, J. E. Lee, S. O. Park, S. Choi, H. K. Kang, and C. Chung, in IEEE International Electron Devices Meeting (2011), pp. 24.1.1–24.1.4.
[62]M. Gajek, J. J. Nowak, J. Z. Sun, P. L. Trouilloud, E. J. O'Sullivan, D. W. Abraham, M. C. Gaidis, G. Hu, S. Brown, Y. Zhu, R. P. Robertazzi, W. J. Gallagher, and D. C. Worledge, Appl. Phys. Lett. 100, 132408 (2012).
[63]H. Sato, M. Yamanouchi, K. Miura, S. Ikeda, R. Koizumi, F. Matsukura, and H. Ohno, IEEE Magn. Lett. 3, 3000204 (2012).
[64]T. Liu, Y. Zhang, J. W. Cai, and H. Y. Pan, Sci. Rep. 4, 5895 (2015).
[65]J.-H. Kim, J.-B. Lee, G.-G. An, S.-M. Yang, W.-S. Chung, H.-S. Park, and J.-P. Hong, Sci. Rep. 5, 16903 (2015).
[66]H. Sato, T. Yamamoto, M. Yamanouchi, S. Ikeda, S. Fukami, K. Kinoshita, F. Matsukura, N. Kasai, and H. Ohno, in IEEE International Electron Devices Meeting (2013), pp. 3.2.1–3.2.4.
[67]E. C. I. Enobio, H. Sato, S. Fukami, F. Matsukura, and H. Ohno, IEEE Magn. Lett. 6, 5700303 (2015).
[68]M. Konoto, H. Imamura, T. Taniguchi, K. Yakushiji, H. Kubota, A. Fukushima, K. Ando, and S. Yuasa, Appl. Phys. Express 6, 073002 (2013).
[69]S. Tsunegi, H. Kubota, S. Tamaru, K. Yakushiji, M. Konoto, A. Fukushima, T. Taniguchi, H. Arai, H. Imamura, and S. Yuasa, Appl. Phys. Express 7, 033004 (2014).
[70]H. Sato, E. C. I. Enobio, M. Yamanouchi, S. Ikeda, S. Fukami, S. Kanai, F. Matsukura, and H. Ohno, Appl. Phys. Lett. 105, 062403 (2014).
[71]S. Ikeda, H. Sato, H. Honjo, E. C. I. Enobio, S. Ishikawa, M. Yamanouchi, S. Fukami, S. Kanai, F. Matsukura, T. Endoh, and H. Ohno, in IEEE International Electron Devices Meeting (2014), pp. 33.2.1–33.2.4.
[72]H. Honjo, H. Sato, S. Ikeda, S. Sato, T. Watanebe, S. Miura, T. Nasuno, Y. Noguchi, M. Yasuhira, T. Tanigawa, H. Koike, M. Muraguchi, M. Niwa, K. Ito, H. Ohno, and T. Endoh, in IEEE Symposium on VLSI Technology (2015), pp. T160–T161.
[73]J. Nowak, R. Robertazzi, J. Sun, G. Hu, J. Park, J. Lee, A. Annunziata, G. Lauer, C. Kothandaraman, E. O. Sullivan, P. Trouilloud, Y. Kim, and D. Worledge, IEEE Magn. Lett. 7, 3102604 (2016).
[74]H. Sato, M. Yamanouchi, S. Ikeda, S. Fukami, F. Matsukura, and H. Ohno, IEEE Trans. Magn. 49, 4437 (2013).
[75]H. Sato, S. Ikeda, S. Fukami, H. Honjo, S. Ishikawa, M. Yamanouchi, K. Mizunuma, F. Matsukura, and H. Ohno, Jpn. J. Appl. Phys., Part 1 53, 04EM02 (2014).
[76]K. Nishioka, H. Honjo, S. Ikeda, T. Watanabe, S. Miura, H. Inoue, T. Tanigawa, Y. Noguchi, M. Yasuhira, H. Sato, and T. Endoh, IEEE Trans. Electron Devices 67, 995 (2020).
[77]A. Hallal, H. X. Yang, B. Dieny, and M. Chshiev, Phys. Rev. B 88, 184423 (2013).
[78]S. Peng, W. Kang, M. Wang, K. Cao, X. Zhao, L. Wang, Y. Zhang, Y. Zhang, Y. Zhou, K. L. Wang, and W. Zhao, IEEE Magn. Lett. 8, 3105805 (2017).
[79]J. Igarashi, J. Llandro, H. Sato, F. Matsukura, and H. Ohno, Appl. Phys. Lett. 111, 132407 (2017).
[80]J.-H. Park, Y. Kim, W. C. Lim, J. H. Kim, S. H. Park, J. H. Kim, W. Kim, K. W. Kim, J. H. Jeong, K. S. Kim, H. Kim, Y. J. Lee, S. C. Oh, J. E. Lee, S. O. Park, S. Watts, D. Apalkov, V. Nikitin, M. Krounbi, S. Jeong, S. Choi, H. K. Kang, and C. Chung, in IEEE Symposium on VLSI Technology (2012), pp. 57–58.
[81]G. Jan, Y.-J. Wang, T. Moriyama, Y.-J. Lee, M. Lin, T. Zhong, R.-Y. Tong, T. Torng, and P.-K. Wang, Appl. Phys. Express 5, 093008 (2012).
[82]L. Thomas, G. Jan, J. Zhu, H. Liu, Y.-J. Lee, S. Le, R.-Y. Tong, K. Pi, Y.-J. Wang, D. Shen, R. He, J. Haq, J. Teng, V. Lam, K. Huang, T. Zhong, T. Torng, and P.-K. Wang, J. Appl. Phys. 115, 172615 (2014).
[83]N. Perrissin, S. Lequeux, N. Strelkov, A. Chavent, L. Vila, L. D. Buda-Prejbeanu, S. Auffret, R. C. Sousa, I. L. Prejbeanu, and B. Dieny, Nanoscale 10, 12187 (2018).

Published under license by AIP Publishing

[84]M. Yamanouchi, R. Koizumi, S. Ikeda, H. Sato, K. Mizunuma, K. Miura, H. D. Gan, F. Matsukura, and H. Ohno, J. Appl. Phys. **109**, 07C712 (2011).
[85]S. Ohuchida, K. Ito, M. Muraguchi, and T. Endoh, in International Conference on Solid State Devices Materials (SSDM) (2015), pp. 1180–1181.
[86]J. M. Shaw, S. E. Russek, T. Thomson, M. J. Donahue, B. D. Terris, O. Hellwig, E. Dobisz, and M. L. Schneider, Phys. Rev. B **78**, 024414 (2008).
[87]T. Shimatsu, H. Kataoka, K. Mitsuzuka, H. Aoi, N. Kikuchi, and O. Kitakami, J. Appl. Phys. **111**, 07B908 (2012).
[88]S. W. Chung, T. Kishi, J. W. Park, M. Yoshikawa, K. S. Park, T. Nagase, K. Sunouchi, H. Kanaya, G. C. Kim, K. Noma, M. S. Lee, A. Yamamoto, K. M. Rho, K. Tsuchida, S. J. Chung, J. Y. Yi, H. S. Kim, Y. S. Chun, H. Oyamatsu, and S. J. Hong, in IEEE International Electron Devices Meeting (2016), pp. 27.1.1–27.1.4.
[89]Y. Huai, H. Gan, Z. Wang, P. Xu, X. Hao, B. K. Yen, R. Malmhall, N. Pakala, C. Wang, J. Zhang, Y. Zhou, D. Jung, K. Satoh, R. Wang, L. Xue, and M. Pakala, Appl. Phys. Lett. **112**, 092402 (2018).
[90]S. Sakhare, M. Perumkunnil, T. H. Bao, S. Rao, W. Kim, D. Crotti, F. Yasin, S. Couet, J. Swerts, S. Kundu, D. Yakimets, R. Baert, H. Oh, A. Spessot, A. Mocuta, G. S. Kar, and A. Furnemont, in IEEE International Electron Devices Meeting (2018), pp. 18.3.1–18.3.4.
[91]L. Thomas, G. Jan, S. Serrano-Guisan, H. Liu, J. Zhu, Y. Lee, S. Le, J. Iwata-Harms, R. Tong, S. Patel, V. Sundar, D. Shen, Y. Yang, R. He, J. Haq, Z. Teng, V. Lam, P. Liu, Y. Wang, T. Zhong, H. Fukuzawa, and P. Wang, in IEEE International Electron Devices Meeting (2018), pp. 27.3.1–27.3.4.
[92]I. M. Miron, K. Garello, G. Gaudin, P. J. Zermatten, M. V. Costache, S. Auffret, S. Bandiera, B. Rodmacq, A. Schuhl, and P. Gambardella, Nature **476**, 189 (2011).
[93]L. Liu, C. F. Pai, Y. Li, H. W. Tseng, D. C. Ralph, and R. A. Buhrman, Science **336**, 555 (2012).
[94]S. Fukami, T. Anekawa, C. Zhang, and H. Ohno, Nat. Nanotechnol. **11**, 621 (2016).
[95]S. Fukami, T. Anekawa, A. Ohkawara, C. Zhang, and H. Ohno, in IEEE Symposium on VLSI Technology (2016), pp. 60–61.
[96]B. Jinnai, C. Zhang, A. Kurenkov, M. Bersweiler, H. Sato, S. Fukami, and H. Ohno, Appl. Phys. Lett. **111**, 102402 (2017).
[97]B. Jinnai, H. Sato, S. Fukami, and H. Ohno, Appl. Phys. Lett. **113**, 212403 (2018).

Published under license by AIP Publishing